

CUT LAYER IN A MACHINING OF THE CYLINDRICAL GEARS BY THE METHOD OF 5-AXIS ROLL AWAY OF THE END MILL CUTTER ON THE OUTLINE OF THE TOOTH

Warstwa skrawana w obróbce walcowych kół zębatych metodą 5-osiowego odtaczania frezu palcowego po zarysie zęba

Michał CHLOST

ORCID 0000-0001-9420-4239

DOI: 10.15199/160.2021.2.5

Abstract: Gear trains are a key element in the transmission of torque and rotational speed of rotating parts. Technological progress, and five-axis machining in particular, is an interesting and still little-known alternative in the production of this type of kinematic nodes in relation to traditional methods. This paper presents the issue and describes the kinematics of the tool operation in an innovative method of shaping five-axis gears by means of the peripheral milling method. The influence of geometry and material on the selection of the tool and its technological parameters was taken into account. A simulation analysis of the cut layer cross-sections and surface topography was carried out. It was shown that the machining direction was of great importance in the described method.

Keywords: gears, hardened machining, 5-axis roll away machining

Streszczenie: Przekładnie zębate w dalszym ciągu stanowią kluczowy element w przenoszeniu momentu oraz prędkości obrotowej części wirujących. Postęp technologiczny, a w szczególności proces obróbki pięcioosiowej na obrabiarkach CNC, stanowi ciekawą i wciąż mało poznaną alternatywę w wytwarzaniu tego typu węzłów kinematycznych w odniesieniu do metod tradycyjnych. W niniejszej pracy przedstawiono problematykę zagadnienia oraz opisano kinematykę pracy narzędzia w nowatorskiej metodzie kształtowania wieloosiowego kół zębatych metodą 5-osiowego odtaczania frezu palcowego po zarysie zęba. Uwzględniono wpływ geometrii oraz materiału przedmiotu obrabianego, na dobór narzędzia oraz jego parametrów pracy. Przeprowadzono badania symulacyjne i analizę warstwy skrawanej oraz topografii powierzchni obrobionej w środowisku CAD/CAM. Pokazano, iż w opisywanej metodzie duże znaczenie ma kierunek obróbki.

Słowa kluczowe: koła zębate, obróbka w stanie utwardzonym, odtaczanie pięcioosiowe

Introduction

Five-axis milling technologies are gaining some increased recognition in the production of elements with advanced geometry, sometimes replacing the methods used so far. The reason for this is the high flexibility of machines and programming of the manufacturing process. It results, among others, from a possibility of controlling the position of the tool in the working space of the machine through displacements in three linear axes, and additionally in two rotary axes. Free positioning of the tool allows reducing the amount of over-clamping of the object, and enables to reduce the tool overhang. This has a positive effect on the stiffness of the machining system, thus increasing the dimensional and shape accuracy of the workpiece after machining [1, 6].

One of the still developing issues in freeform milling is a possibility of making toothings of gears. The techniques of classic gear machining used so far are based on the use of specialized machine tools and dedicated tools. The kinematics of the manufacturing process in this case consists in rolling away the tool around the envelope in order to shape the involute profile [6, 11, 14]. This process

results in simultaneous processing of both the right and left sides of the tooth, which ensures high efficiency of the process, but does not allow individual shaping of each of the surfaces machined. The detailed analysis of chip formation in hobbing was performed by Bouzakis et al. [4], and Krömer et al. [13] described the process in terms of the obtained roughness R_{th} in the direction of the line and the tooth profile. Additional analyzes in the case of the innovative skiving method described by Davim [7] were carried out by Böß et al. [3, 2] where they analyzed cross-section values of the cutting layer depended on the position of the tool cutting edge.

A completely different approach to the issue of gear manufacturing is the use of five-axis machining methods on multi-axis CNC machine tools. When shaping elements using this process, two basic technological variants of tool guidance are distinguished: machining with a point contact and machining of the cutter's side with a linear contact. In the works [10, 12, 15, 16, 19] the linear contact was obtained by tangential positioning of the tool surface at the point of its corner or transition to a spherical face, to the tooth side contour curve. A different machining kinematics was adopted by Talar et al. [18], who

carried out an analysis of multi-axis cutting using a disc head for machining, where the contact of the tool with the machined tooth side surface was also unchanged, and moreover based on the transition point of the linear cutting edge of the insert into the corner radius.

Depending on the method adopted, the cross-sectional area of the cutting layer changes, which has a significant impact on the values of the cutting force components in the milling process. In the case of the envelope machining, the method of determining the cross-sectional area of the cut layer was shown by Bouzakis et al. [4] and Böß et al. [2, 3]. In the process of five-axis milling in the variant with point contact, the methodology of determining the cross-sectional area of the cut layer was presented by Boz et al. [5], and with the use of a toroidal milling cutter by Gdula et al. [9]. For the linear contact, the problem of the cut layer cross-section was discussed by Talar et al. [18].

The last element influencing the correct collaboration of the tooth active surfaces in the gear is the machined surface texture. The basic types of machining marks obtained in the envelope processes were presented by Sun et al. [17]. In addition, Kromer et al. [13] and Piotrowski et al. [14], performed an analysis of the machined surface after hobbing. The geometry of the tooth side surface after five-axis shaping in the variant of point contact was presented by Klocke et al. [12] and Staudt et al. [16].

This article presents an analysis of the cross-sections of the cut layer in the new proposed method of machining the toothing by the 5-axis roll away of the end mill along the involute contour of the tooth side of a wheel with a cylindrical geometry. The assumption is the continuous and controlled movement of the contact point of the tool and the workpiece along the outline of tool. (Fig. 1.) shows the idea of the process, i.e. inscribing a monolithic tool into the outline of a tool for envelope machining, which in the analyzed case is represented by the MAAG rack cutter.

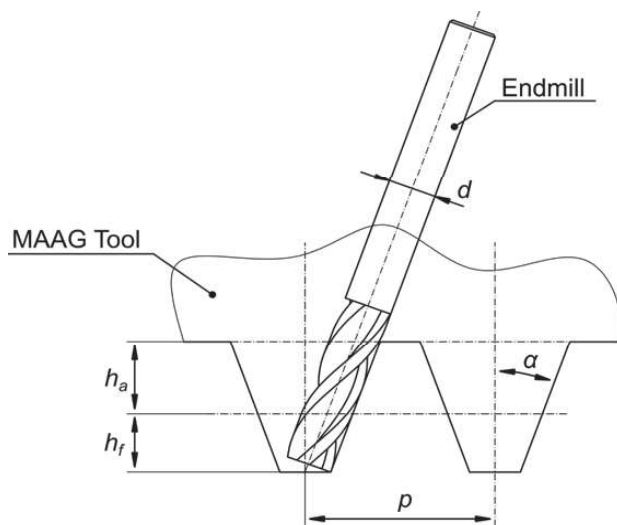


Fig. 1. The idea of a five-axis roll away process

Materials and methods

The simulation of the machining of the gear tooth flank was carried out for an involute contour, delimited by the based circle and the addendum circle. The simulation omits the transition curve at the root of teeth, whose processing due to the geometry, requires the use of a ball end mill end, and in the five-axis milling process it can be performed in a separate operation.

The tool feed rate v_f was adopted along the tooth profile, as a result of which the involute curve was divided into segments whose length corresponds to the adopted tool feed per revolution f . Two machining cases were considered. In the first case, the tool runs from the root to the tooth top (Fig. 2.), while in the second, the direction of the feed rate speed v_f and the rolling movement are changed, so that the machining proceeds from the top to the tooth root.

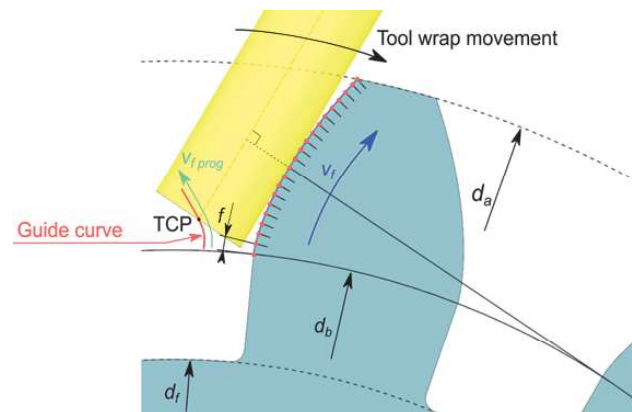


Fig. 2. Tool work kinematics

In the simulation, the tool positions were determined geometrically, as positions tangent to the involute at points determined by the value of the feed per revolution f . In real machining, the tool path represented by the TCP point will be based on the guide curve resulting from rolling away the tool around the contour, and the tool feedrate will be converted from the speed on the involute profile v_f to the speed along the guide curve $v_{f \text{ prog}}$.

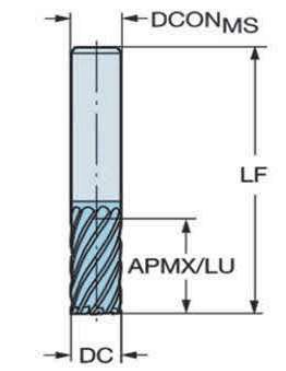
The cross-section analysis of the cut layer in the new five-axis turning method was carried out for the adopted material and technological parameters. The hardened 40HM steel was used as the material, for which the hardness was 60 HRC, and the mechanical properties are presented in Tab. 1. The selection of the steel grade was dictated by its susceptibility to mechanical and heat treatment.

Table 1. 40 HM steel properties [8]

Density ρ g/cm ³	Young's modulus E GPa	Tensile strength Rm MPa	Yield strength R _{p0.2} MPa	Elongation A %	Hardness HRC
7.82	205 - 210	1030	880	10	60

Using material from the H group, i.e. the material with increased strength, it became necessary to choose the right tool for processing this type of material. In this case, a Sandvik tool with the parameters shown in Tab. 2 was selected.

Table 2. Tool geometry

	R215.38-08030-AC19H 1610	
	DC mm	8
	APMX/LU mm	19
	LF mm	63
	DCONMS mm	8

According to catalogue notes, for the selected tool, the technological parameters of machining proposed by the manufacturer and described in Tab. 3 were adopted.

Table 3. Technological parameters

Cutting speed v_c m/min	Feed per revolution f mm/rev	Cutting width a_{emax} mm	Cutting depth a_{pmax} mm
80	0.8	0.05 DC	1.5 DC

The quantities having a significant impact on the selection of the tool geometry, in addition to the material used, were the geometrical parameters of the workpiece, which is the gear wheel. First of all, the width of the space s , which influences the maximum diameter DC of the tool, as well as the length of the involute profile L_{inv} of the tooth, which is important when selecting the maximum useful depth of cut $APMAX/LU$ of the tool, were taken into account. The main parameters of the machined gear are presented in Tab. 4.

Table 4. Gear parameters

Pressure angle α °	Modulus m_n mm	Teeth number z -	Helix angle β °	Involute length L_{inv} mm	Space width s mm
20	10	14	0	15.7589	15.707

The values in the above table were determined as follows. The length of the involute curve is described by the equation (1),

$$L_{inv} = \int_0^t \sqrt{\left(\frac{dx}{dt}\right)^2 + \left(\frac{dy}{dt}\right)^2} \quad (1)$$

where the derivatives after the variable t refer to the functions expressed by equation (2). In this case, the variable t represents the involute angle.

$$\begin{cases} x(t) = \frac{d_b}{2} (\sin(t) - t \cos(t)) \\ y(t) = \frac{d_b}{2} (\cos(t) + t \sin(t)) \end{cases} \quad (2)$$

In equations (2) there is a variable d_b which is the diameter of the base circle and is expressed by equation (3).

$$d_b = d_p \cos(\alpha) = m_n z \cos(\alpha) \quad (3)$$

The value of the width of the space s was determined using the equation (4).

$$s = \frac{\pi m_n}{2} \quad (4)$$

The study of the cross-sections of the cut layers was carried out in 4 separate cutting zones towards the tooth line. The zones were determined on the basis of the tool wrap angle analysis. One can distinguish: entrance zone I, stable cutting zone II, output zone N-1, and the last cut of the tool N (Fig. 3.). The analysis was carried out in representative zones, while the total number of cutting zones is determined by the parameter N, which is calculated from the formula (5)

$$N = \frac{b}{b_r} + 1 \quad (5)$$

where: b - gear width, b_r - distance between next passes of the tool. For the purposes of the study, the b_r parameter was assumed to be 1 mm.

Each zone is characterized by a different value of the wrap angle of the tool. The determination of the wrap angle in individual zones was important for the correct division of the cutting zone in order to analyze the cross-section area of the cut layer A.

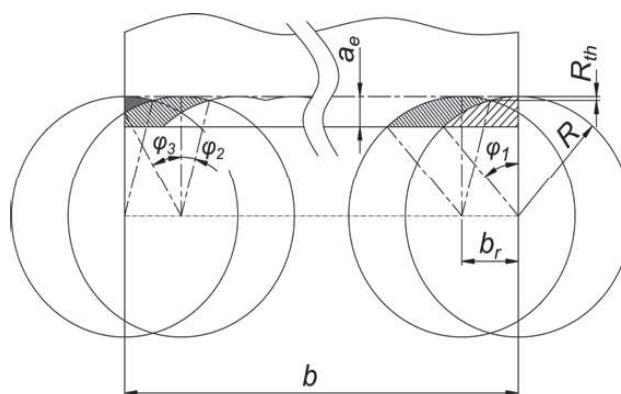


Fig. 3. Tool wrap angles in designated zones

The values of the wrap angles, determined by equations (5-8), in the separate zones are described as sums of partial angles.

$$\varphi_I = \varphi_1 \quad (5)$$

$$\varphi_{II} = \varphi_1 + \varphi_2 \quad (6)$$

$$\varphi_{N-1} = \varphi_2 + \varphi_3 \quad (7)$$

$$\varphi_N = \varphi_2 \quad (8)$$

The partial angles that make up the wrap angles of tool are described by equations (9-11)

$$\varphi_1 = \tan^{-1} \left(\frac{R^2 - (R - a_e)^2 - br}{R - a_e} \right) \quad (9)$$

$$\varphi_2 = \tan^{-1} \left(\frac{\frac{b_r}{2}}{R - R_{th}} \right) \quad (10)$$

$$\varphi_3 = \sin^{-1} \left(\frac{b_r}{R} \right) \quad (11)$$

where: R - tool radius, a_e - cutting width (machining allowance), b_r - width between next passes of the tool, R_{th} - theoretical roughness in the direction of the tooth line expressed by the formula (12).

$$R_{th} = R - \sqrt{R^2 - \left(\frac{b_r}{2}\right)^2} \quad (12)$$

In order to thoroughly analyze the cutting layers A , as well as to determine the total cross-sectional area of the cutting layers A_z , the wrap angles were discretized with a step $\Delta\varphi$ equal to 2° from the 0° position, i.e. the plane normal to the machined surface, passing through the tool axis. Due to the irrationality of the wrap angles value, the last step was taken as the remainder from the division $\pm\varphi$ as shown in (Fig. 4.).

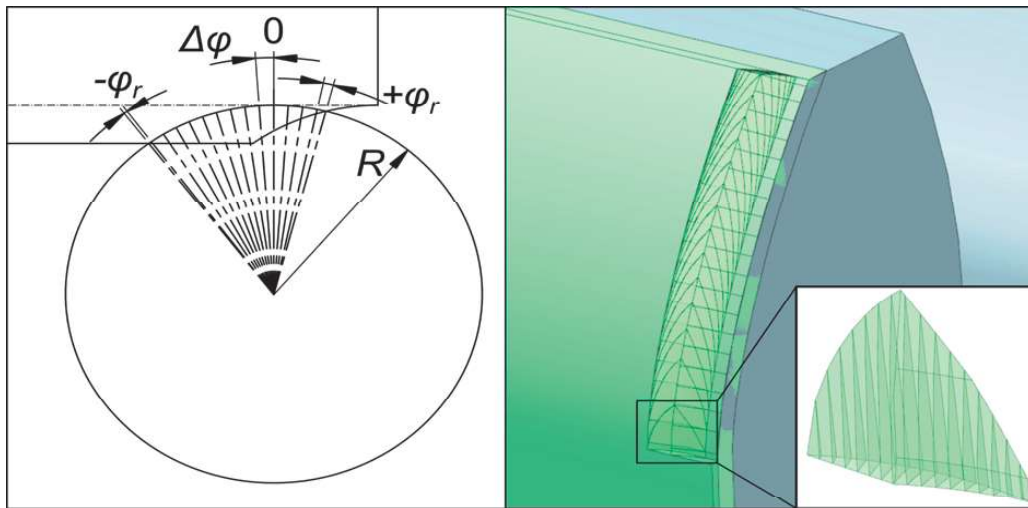


Fig. 4. Cutting zone discretization

Results

Due to the complex geometry of the cutting layer, the measurement of individual sections A was carried out using the Measure Face tool, which is part of the NX11 software. The accuracy of the measurement was $\pm 0.0001 \text{ mm}^2$.

Figures 5-8 show the change in the value of the cross-sectional area of the cutting layer A depending on the wrap angle φ for the strategy in which the tool works from the top to the tooth root. The analysis of the graphs shows that the highest value of the cross-sectional area was obtained in zone I, as shown in (Fig. 5.). In this case, it can be clearly observed that the largest cross-sectional area of the cutting layer $A = 1.5148 \text{ mm}^2$ occurs at the first position of the tool, i.e. at the tooth top for the angular position of 0° .

The smallest values of the cross-sectional area A were observed for the zone N-1 (Fig. 8.), where the maximum value was $A = 0.2807 \text{ mm}^2$. The waveforms for the zones II and N-1 are characterized by the same maximum values of $A = 1.0613 \text{ mm}^2$, but with a variable slope of the left side of the plot (Figures 6-7). Three areas can be noticed on all the waveforms showing the change in the cross-section of the cut layer depending on the considered tool position on the involute curve. The area of the tool entry into the material in the range 1-2, where there is the largest cross-sectional area A , the stable cutting zone, which for zone I is within the limits of 2-16, for zone II and zone N-1 within the border 2-17, and for zone N within the limits 2-18. In addition, the cutting area with the face cutting of the tool was separated, where the value of the cross-sectional area of the cut layer decreases.

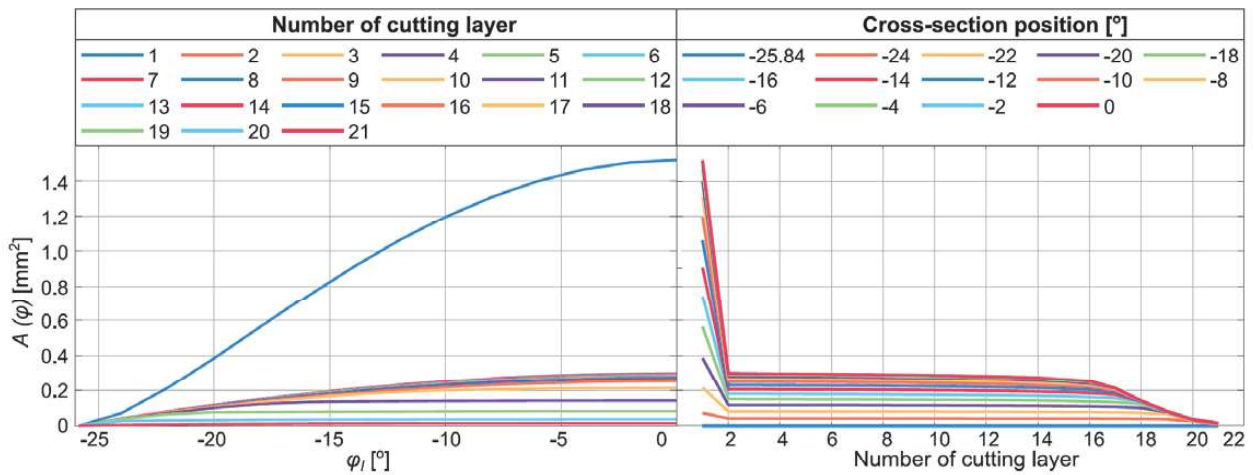


Fig. 5. The cross-sectional areas of the cut layer in zone I

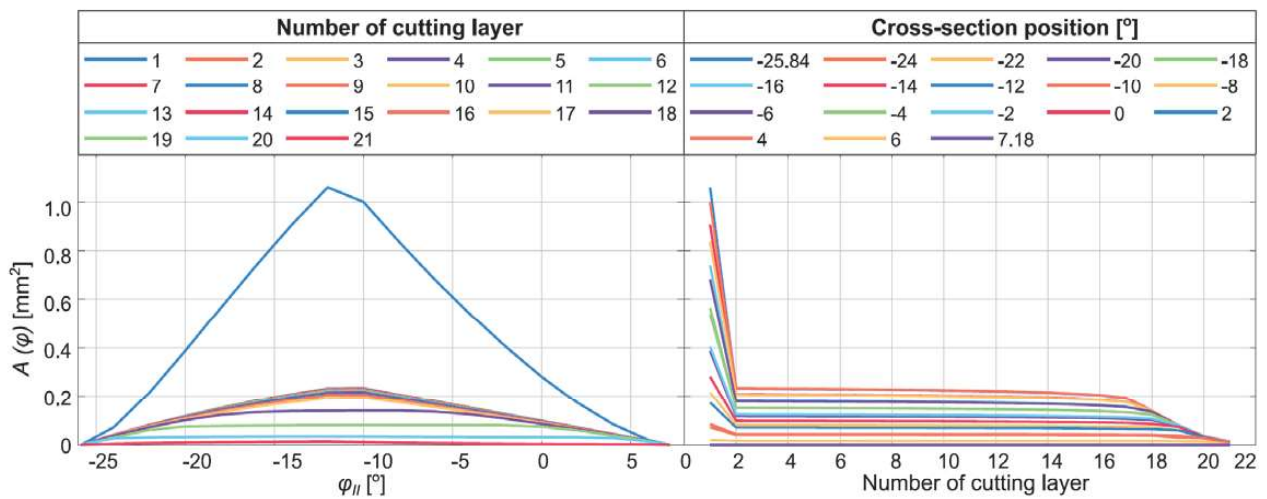


Fig. 6. The cross-sectional areas of the cut layer in zone II

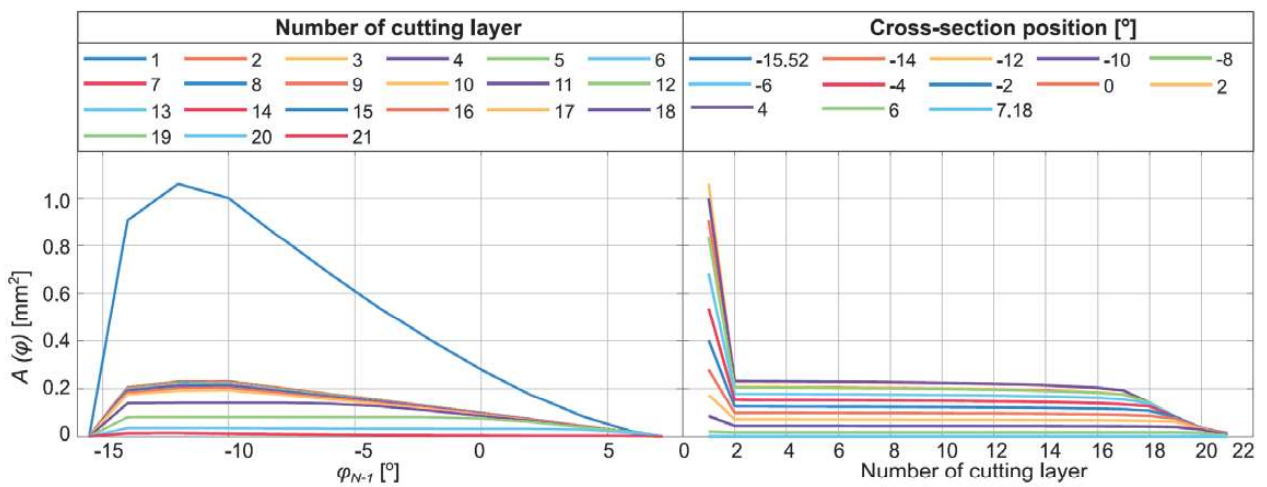


Fig. 7. The cross-sectional areas of the cut layer in zone N-1

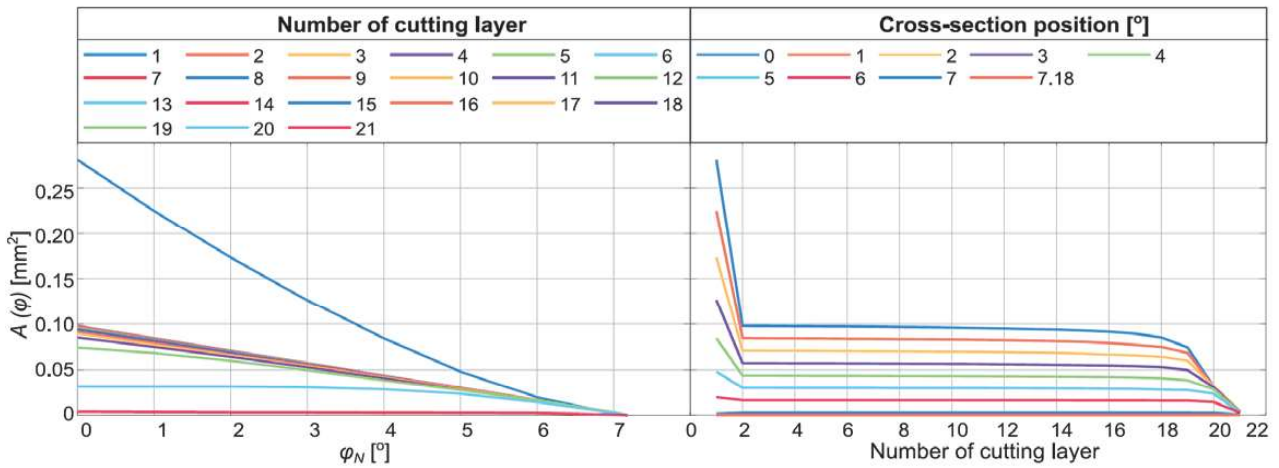


Fig. 8. The cross-sectional areas of the cut layer in zone N

The analysis of the milling strategy from the root to the top of the tooth showed some differences as seen in (Figures 9.-11.). A similar distribution of maximum values for individual zones was observed, as in the previous strategy. In this case, for zone I, the highest maximum

value of the cross-sectional area $A = 0.6652 \text{ mm}^2$ (Fig. 9.) was recorded, and the smallest for zone N, which was $A = 0.174 \text{ mm}^2$ Fig 12. In the case of zones II and N-1 of (Figures 10.-11.), the same maximum values of $A =$

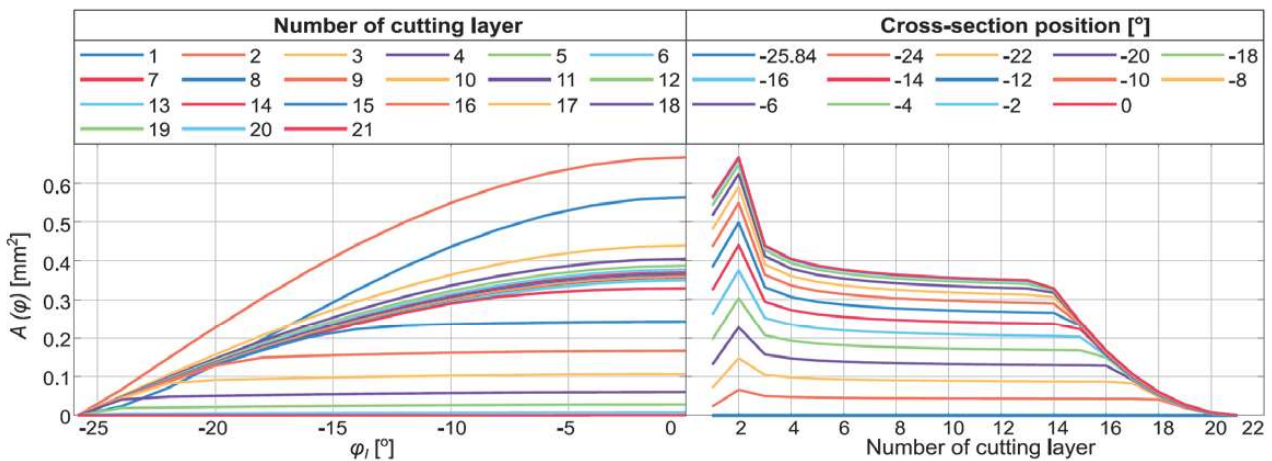


Fig. 9. The cross-sectional areas of the cut layer in zone I

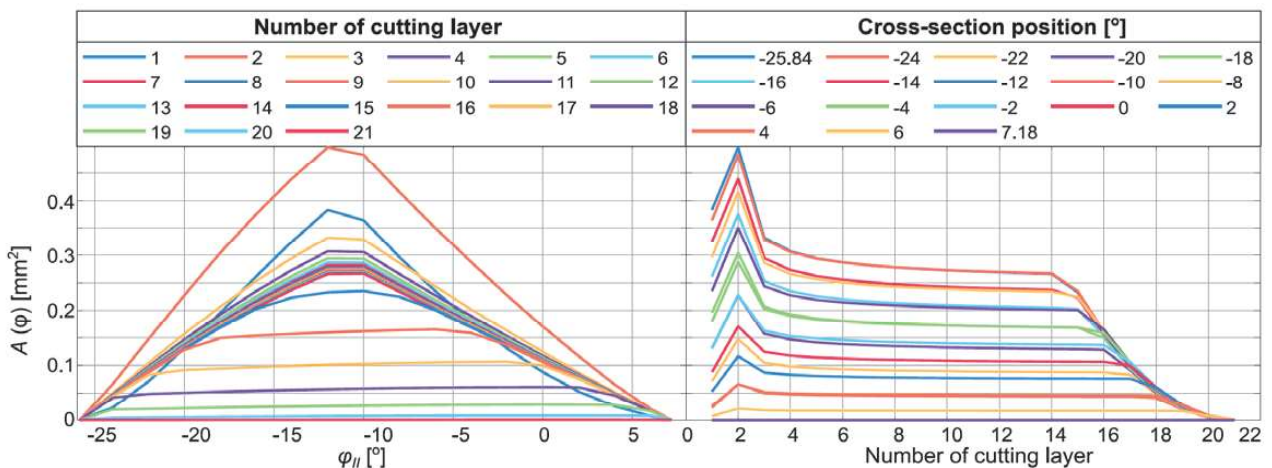


Fig. 10. The cross-sectional areas of the cut layer in zone II

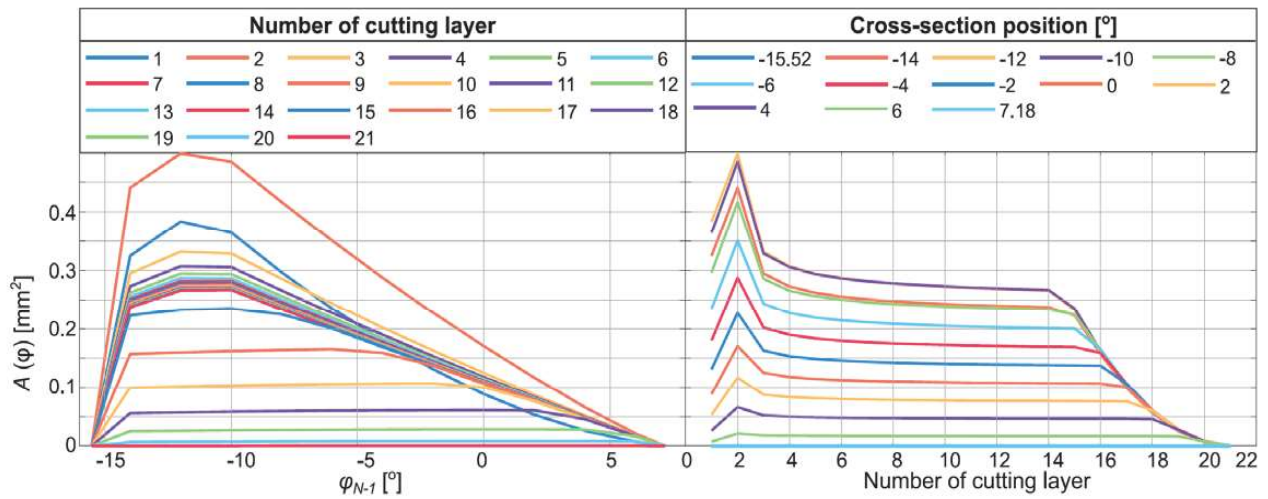


Fig. 11. The cross-sectional areas of the cut layer in zone N-1

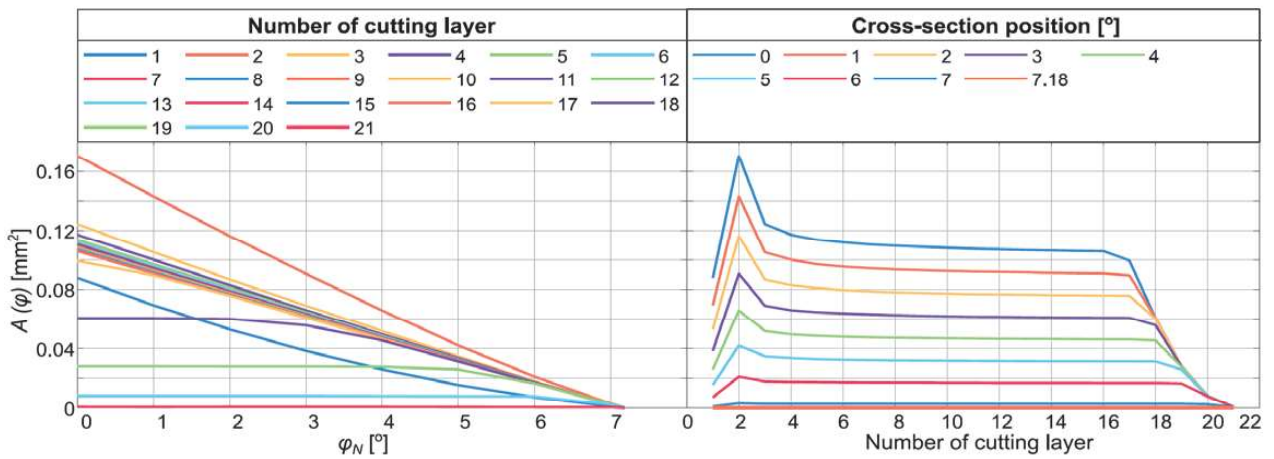


Fig. 12. The cross-sectional areas of the cut layer in zone N

0.4981 mm² and a similar change in the slope of the left side of the plot were observed.

The main difference was observed in the changes of the cross-sectional area depending on the position of the tool. The area of the tool entry into the material covers the positions 1-3, where the maximum value was noted for the position 2. The stable cutting area for zone I ranges from 2-13, for zones II and N-1 it ranges from 2-14, and for N z...

from the material, in which the cross-section of the cutting layer decreases in the case under consideration, has a wider range than in the previous strategy.

Based on the above data, graphs of the total cross-sectional area of the cutting layers A_z in individual zones were prepared for the milling strategy from the top to the root of the tooth (Fig. 13.), and from the root to the top of the tooth (Fig. 14.).

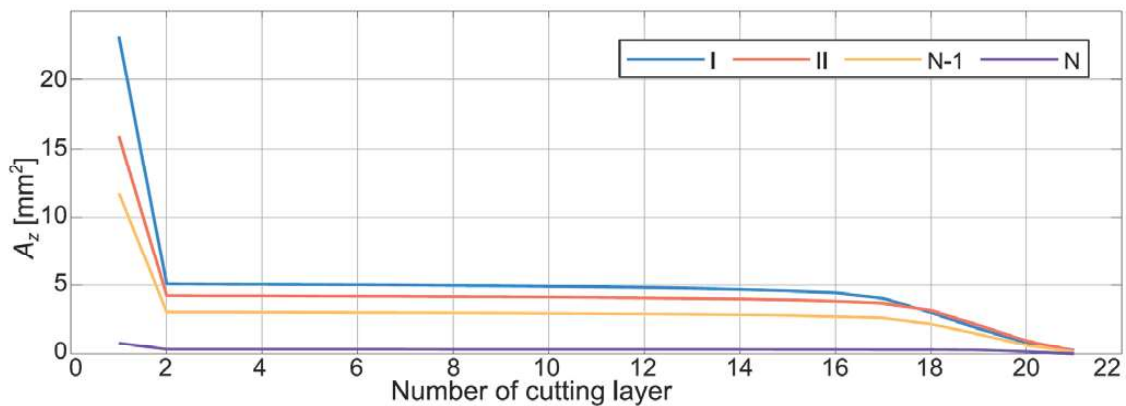


Fig. 13. The total cross-sectional area of the cutting layers for the direction from top to tooth root

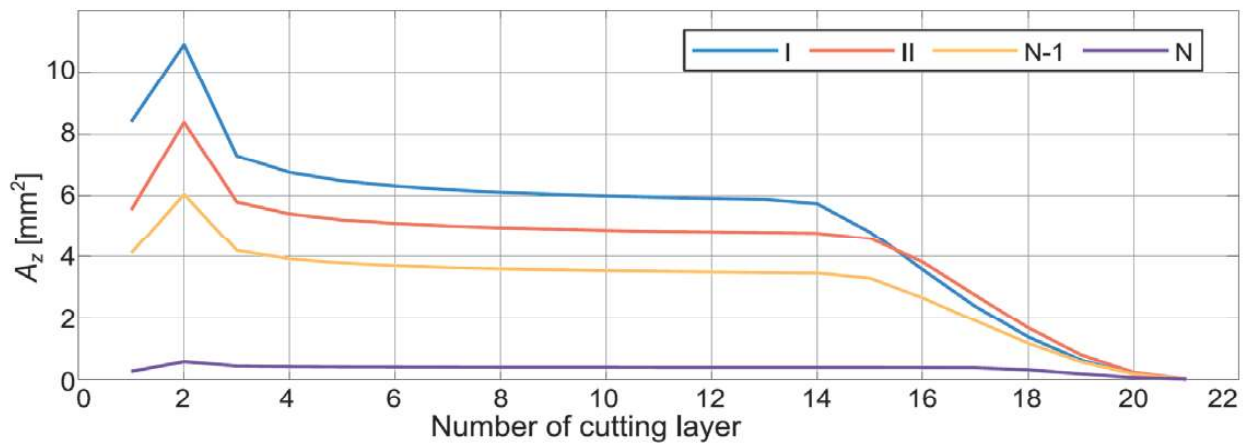


Fig. 14. The total cross-sectional area of the cutting layers for the direction from root to tooth top

For all four zones (I, II, N-1, N), the total cross-sectional area A_z was calculated as the sum of the cross-sections $A(\varphi)$ at individual positions of the tool, which is expressed by the general formula (13)

$$A_z = \sum_{i=1}^n A(\varphi)_i \quad (13)$$

where: n – number of cross-section position.

It was observed, that in the case of the root to tooth top strategy, the obtained values of the total A_z cross-sectional areas were about half lower than those obtained in the top to tooth root strategy. Moreover, the highest

values occurred for the zone I, and the lowest for the zone N. The nature of the change in the total values of the cross-section areas A_z for individual zones and strategies coincides with the previously discussed results for the cross-section areas A .

The last element of the analysis was the presentation of a map of surface deviations depending on the adopted machining direction (Figures 15a, b.) The maximum deviation in both cases coincided with the theoretical roughness towards the tooth line expressed by the formula (12) and amounted to 0.0314 mm. It was observed that the machining marks arranged up along the tooth profile, while the deviation for individual marks took the saddle, biconcave character (Fig. 15c.).

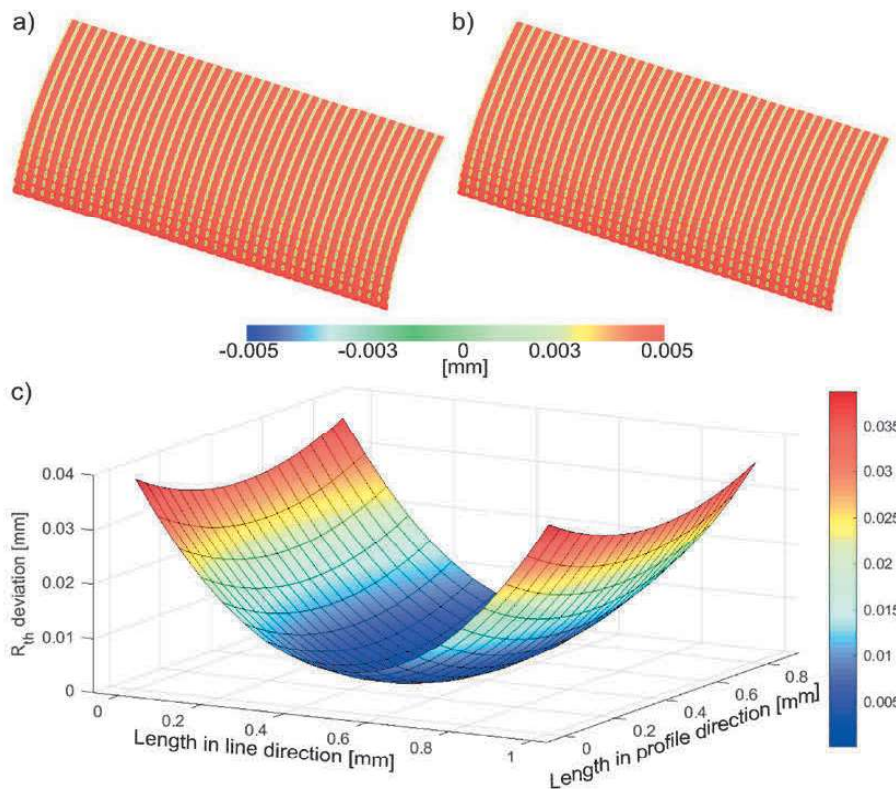


Fig. 15. Map of surface deviations for: a) root-top strategy, b) top-root strategy, c) deviation distribution for one cut layer

Summary

The analyzed milling method in the technological variant of 5-axis roll away of the end mill cutter is a completely new look at the issue of five-axis gear machining. Simulation tests and the analysis of the cross-sections of the cut layers showed a different distribution of values along the tooth profile depending on the adopted machining direction.

The values of the cross-sectional areas of the cut layers have a particular impact on the values of the components of the cutting forces generated during machining, and thus on the deformation of the machining system.

On the basis of the results obtained, it should be concluded that:

- The machining from the root to the tooth's top will be a more advantageous strategy due to the smaller values of the cross-sections of the cut layers. In this case, the greatest value of the cross-sectional area is noted at the root of the tooth.
- In the case of the top to tooth root strategy, the cross-sectional area values are more than twice as high. Moreover, in this case, the largest cross-sectional area is recorded in the first position, i.e. at the top of the tooth. Such a distribution of values can result in the application of the greatest resultant cutting force to the area of the tooth top, thus deforming both the tool and the workpiece.

The results and conclusions obtained from the conducted analyzes provide the basis for further research on the five-axis roll away process. In the next steps, one should focus on:

- Developing the control program by replacing the feed along the involute curve v_f with the feed along the guide curve $v_f \text{ prog}$.
- The values of the cross-sectional areas A should be made dependent on the parameters: feed per revolution f , cutting width a_e and the distance between tool paths b_r .
- In the case of the adopted method of finishing the material in the hardened state, it will be necessary to precisely determine the maximum cross-sections for individual cut layers A_{\max} and to analyze the components of the cutting force.

References

- [1] Álvarez, ÁI., A. Calleja, M. Arizmendi, H. González, and L. de Lacalle. 2018. "Spiral Bevel Gears Face Roughness Prediction Produced by CNC End Milling Centers." *Materials* 11 (8).
- [2] Böß, V., B. Denkena, M. Dittrich, and S. Henning. 2016. "Geometrical Contact Zone Analysis of the Skive Hobbing Process." *Advanced Materials Research* 1140: 157–64.
- [3] Böß, V., B. Denkena, and S. Henning. 2015. "Investigation of the Skive Hobbing Process by Applying a Dexcel-Based Cutting Simulation." *Procedia CIRP* 37: 182–87.
- [4] Bouzakis, K. D., E. Lili, N. Michailidis, and O. Frideirikos. 2008. "Manufacturing of Cylindrical Gears by Generating Cutting Processes: A Critical Synthesis of Analysis Methods." *CIRP Annals - Manufacturing Technology* 57 (2): 676–96.
- [5] Boz, Y., H. Erdim, and I. Lazoglu. 2011. "Modeling Cutting Forces for Five Axis Milling of Sculptured Surfaces." *Advanced Materials Research* 223 (April): 701–12.
- [6] Burek, J., M. Gdula, M. Płodzień, and J. Buk. 2015. "Gear's Tooth Profile Shaping in Dialog and Parametric Programming." *Mechanik*, no. February (February): 142/7.
- [7] Davim, J. 2011. *Machining of Hard Materials*. Machining of Hard Materials.
- [8] Dobrzański, L. A. 2006. "Stale i Inne Stopy Żelaza." In *Podstawy Nauki o Materiałach i Metaloznawstwo*, 591–92. Warszawa: Wydawnictwo Naukowo-Techniczne.
- [9] Gdula, M., and J. Burek. 2017. "Cutting Layer and Cutting Forces in a 5-Axis Milling of Sculptured Surfaces Using the Toroidal Cutter." *Journal of Machine Engineering* 17 (4): 98–122.
- [10] Guo, E., N. Ren, Z. Liu, X. Zheng, and C. Zhou. 2019. "Study on Tooth Profile Error of Cylindrical Gears Manufactured by Flexible Free-Form Milling." *The International Journal of Advanced Manufacturing Technology* 103: 4443–51.
- [11] Karpuschewski, B., H. J. Knoche, and M. Hipke. 2008. "Gear Finishing by Abrasive Processes." *CIRP Annals - Manufacturing Technology* 57 (2): 621–40.
- [12] Klocke, F., M. Brumm, and J. Staudt. 2015. "Quality and Surface of Gears Manufactured by Free-Form Milling with Standard Tools." *Gear Technology*, no. January/February: 64–69.
- [13] Krömer, M., D. Sari, C. Löpenhaus, and C. Brecher. 2017. "Surface Characteristics of Hobbed Gears." *Gear Technology*, no. July: 68–75.
- [14] Piotrowski, A., and T. Nieszporek. 2012. "GRANIASTOŚĆ POWIERZCHNI ZĘBA KOŁA WALCOWEGO PRZY FREZOWANIU OBWIĘDNIOWYM THE LOBBING OF THE TOOTH OF THE SPOOR GEAR AT HOBGING." *Mechanik* 85 (7CD): 795–806.
- [15] Solf, M., R. Bieker, C. Löpenhaus, F. Klocke, and T. Bergs. 2019. "Influence of the Machining Strategy on the Resulting Properties of Five-Axis Hard-Milled Bevel Gears." *Proceedings of the Institution of Mechanical Engineers, Part C: Journal of Mechanical Engineering Science* 233 (21–22): 7358–67.
- [16] Staudt, J., C. Löpenhaus, and F. Klocke. 2017. "Performance of Gears Manufactured by 5-Axis Milling," no. April: 58–65.
- [17] Sun, W., and A. Lancaster. 2017. *Surface Texture Measurements of Gear Surfaces Using Stylus Instruments*. National Physical Laboratory, Vol. 147.
- [18] Talar, R., P. Jablonski, and W. Ptaszynski. 2018. "New Method of Machining Teeth on Unspecialised Machine Tools." *Tehnicki Vjesnik* 25 (1): 80–87.
- [19] Xiang, T., J. Yi, and W. Li. 2018. "Five-Axis Numerical Control Machining of the Tooth Flank of a Logarithmic Spiral Bevel Gear Pinion." *Transactions of Famena* 42 (1): 73–84.

Mgr inż. Michał Chlost
Rzeszów University of Technology,
Faculty of Mechanical Engineering and Aeronautics,
Department of Manufacturing Techniques and
Automation
ul. Wincentego Pola 2, 35-959 Rzeszów, Poland
e-mail: m.chlost@prz.edu.pl